EFFECT OF INTERDIFFUSION ON BAND STRUCTURE IN GAAS/$GA_{1-X}AL_XAS$ QUANTUM RING SUPERLATTICES

Vram MUGHNETSYAN[1], Albert KIRAKOSYAN[2], Aram MANASELYAN[3],

Department of Solid State Physics, Yerevan State University, Al. Manookian 1, 0025 Yerevan, Armenia,

e-mail adresses: [1]vram@ysu.am, [2]kirakosyan@ysu.am, [3]amanasel@ysu.am

Abstract

The effect of interdiffusion on band structure of superlattices composed of initially cylindrical GaAs/$Ga_{1-x}Al_xAs$ quantum rings is investigated. Two cases of superlattices, namely, a three dimensional superlattice composed of Gaussian-shaped double quantum rings and one layer quantum ring superlattice are considered. The Fourier transformation to momentum space is used to solve the Schrödinger equation. In the case of one layer superlattice the adiabatic approximation is also used to take into consideration the transversal motion of electron. It is shown that due to interdiffusion both the first and the second minibands of conduction band shift to the region of higher energies and broaden. The cylindrical symmetry of rings as well as the difference between the behaviors of the dispersion curves in different directions of momentum space gradually disappears. The obtained results indicate to the opportunity of purposeful manipulation of structure characteristics by means of interdiffusion both quantitively and qualitatively.
Keywords: Quantum Ring Superlattice, Interdiffusion, Electronic States, Bloch Amplitudes

INTRODUCTION

Quantum rings (QR) are of great interest due to their unique electronic, magnetic, and optical properties [1]–[2]. For example, quantum phase coherence effects on carrier transport such as in the Aharonov-Bohm and Aharonov-Casher effects are observed in QRs [3]. Some research groups have predicted and demonstrated the optical Aharonov-Bohm effect which may lead to potential applications in quantum information systems [4]–[6]. QRs have also found use in various practical applications in the last few years. Photodetectors based on semiconductor nanorings have been fabricated in the mid-infrared and THz spectral ranges [7],[8]. The potential application in nano-devices has given rise to theoretical investigation and prediction of optoelectronic properties of QRs taking into account the influences of spin-orbit coupling, hydrostatic pressure and polaronic effects [9]-[11]. Analytical treatments of one and two electronic states in QRs with non-trivial geometry has also been suggested [12],[13]. During the last decade impressive progress has been made in the field of manufacturing of ordered structures composed of two- or three-dimensional arrays of QRs [14]-[16]. Recently the arrays of strain-free GaAs/$Al_{0.33}Ga_{0.67}As$ QRs have been fabricated by droplet epitaxy [15]. It is shown that the rapid thermal annealing (RTA) plays a major role in modifying the electronic structure and in the improvement of material quality. In this regard the investigation of the interdiffusion between the compound materials of heterostructure induced by post growth RTA is of great interest. There are promising results, concerning to the application of interdiffusion in order to construct devices with controlling parameters [17]–[20]. Theoretical calculations [21],[22] indicate to the increase of absorption threshold of quantum dots due to interdiffusion, which is in accordance with the experimentally observed blue shift of photoluminescence spectrum [20].

In this work the effect of interdiffusion of Al and Ga atoms on confining potential, and the band structure of three dimensional superlattice (SL) composed of Gaussian-shaped GaAs/$Ga_{1-x}Al_xAs$ double QRs and one-layer QR SL is investigated in the framework of adiabatic approximation and using the Fourier transformation to momentum space.

1. CONDUCTION BAND CONFINING POTENTIAL

Let us introduce the shape function of QR following to Gunawan et. al. [23]:

$$f(\rho,z)=\begin{cases}1, & 0\le z\le z_0(\rho),\\ 0, & z<0 \text{ or } z>z_0(\rho),\end{cases} \tag{1}$$

where

$$z_0(\rho)=A\exp(-\alpha^2(\rho-\rho_1)^2)+B\exp(-\beta^2(\rho-\rho_2)^2)\,. \tag{2}$$

for Gaussian-shaped double QR (GSDQR), and

$$z_0(\rho)=H\cdot\theta(d/2-|\rho-\rho_0|) \tag{3}$$

for QR with rectangular profile. Here A, B, α and β are the Gaussian parameters, ρ_1 and ρ_2 are the average radiuses of the inner and the outer rings of GSDQR respectively, ρ_0, H and d are the average radius, height and the width, respectively, of the single ring with the rectangular profile, $\theta(x)$ is the unite step function. Assuming that before the interdiffusion there are no Al atoms in the region of QRs and the concentration of Al atoms is constant (X_0) elsewhere one can solve the diffusion equation which leads to the following expressions for the Al concentration: for GSDQR SL

$$X(x,y,z;L)=X_0\left\{1-\sum_{\vec{R}}\left(\frac{erf(\tau_z/L)}{2}+\mathrm{e}^{-(\tau_\rho/L)^2}\int_0^\infty\frac{x}{L^2}\mathrm{e}^{-(x/L)^2}I_0\left(\frac{2\tau_\rho x}{L^2}\right)erf\left(\frac{z_0(x)-\tau_z}{L}\right)dx\right)\right\}, \tag{4}$$

where $L=2\sqrt{Dt}$ is the diffusion parameter, D is the diffusion coefficient, t is time, $\tau_\rho=\sqrt{(x-R_x)^2+(y-R_y)^2}$, $\tau_z=z-R_z$, $\vec{R}$ is the radial vector of the center of corresponding QR base, $erf(q)$ is the error function and $I_0(q)$ is the modified Bessel function of zero order, and for one layer QR SL

$$X(\vec{\rho},L)=X_0\left\{1-\frac{2}{L^2}\sum_{\vec{R}}e^{-\tau_\rho^2/L^2}\int_{R_1}^{R_2}\alpha e^{-\alpha^2/L^2}I_0\left(2\tau_\rho\alpha/L^2\right)d\alpha\right\} \tag{5}$$

where R_1 and R_2 are the inner and the outer radii of QR respectively. The potential profile in conduction band is proportinal to the Al concentration:

$$V(\vec{r},L)=QqX(\vec{r},L)\,, \tag{6}$$

where $Q=0.6$ is conduction band offset and $q=1247meV$ for GaAlAs structure.

In Fig.1 the potential cross sections by $z=0.1a$ and $x=0$ planes are illustrated for GSDQR SL of cubic symmetry ($a_x=a_y=a_z=a$) at the values of parameters $A=B=\rho_2=2\rho_1=a/3$, $\alpha=\beta=25/a$. It is clear that for smaller values of diffusion length ($L/a=0.03$ and $L/a=0.1$) the potentials of separate GSDQRs retains cylindrical symmetry (see the upper row of graphics), while for enough large values of diffusion length the rectangular symmetry of superlattice superimpose on the cylindrical symmetry of GSDQR. One can also see that the potential barriers in the center and between the concentric rings decrease with the increase of L and finally vanish (at $L/a=0.2$). The same features can be observed for the potential cross section by the $x=0$ plane. Namely the abrupt profile smoothes out, the barriers between the concentric rings (for $L/a=0.03$ and $L/a=0.1$) and further the central barrier (for $L/a=0.2$) gradually decrease and vanish. A

similar situation is observed for the potential profile of OLQR SL so we do not present here the detailes for this case.

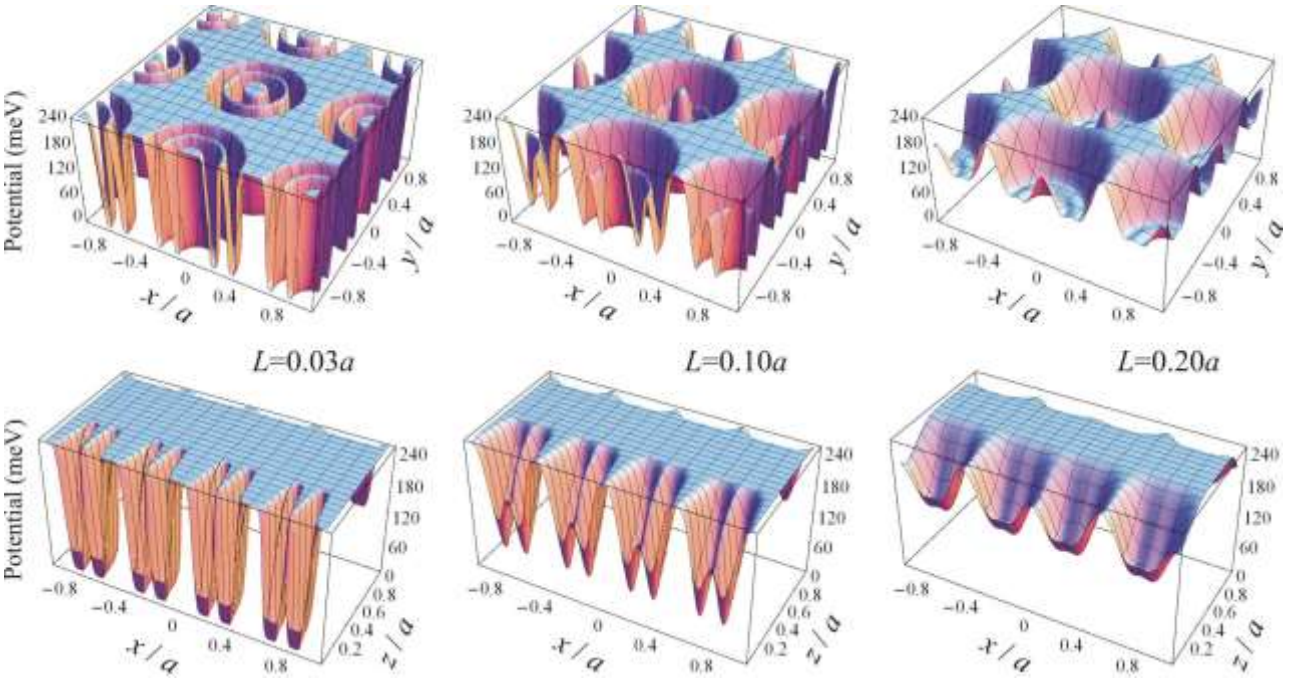

Fig. 1 The dependences of confining potential of GSDQR SL of cubic symmetry with lattice constant a on x and y coordinates for $z = 0.1a$ (the upper row of graphics) and on x and z coordinates for $y = 0$ (the lower row)

2. BAND STRUCTURE

Following to the method developed by Gunawan et al. [22] for periodic potentials, we present the wave function, the reciprocal effective mass and the confining potential in the form of Fourier series:

$$\psi(\vec{\rho}) = \sum_{\vec{g}} u_{\vec{g}} e^{i(\vec{k}+\vec{g})\vec{\rho}}, \qquad \frac{1}{m(\vec{\rho};L)} = \sum_{\vec{g}} m_{\vec{g}}^{-1} e^{i\vec{g}\vec{\rho}}, \qquad V(\vec{\rho},L) = \sum_{\vec{g}} V_{\vec{g}} e^{i\vec{g}\vec{\rho}}, \tag{7}$$

where $\vec{g}$ is the reciprocal lattice vector, $\vec{k}$ is the quasimomentum. In the case of three dimensional SL the summations in Eq. (7) are carried out by the three dimensional vectors $\vec{g}$, while for one layer QR SL $\vec{g}$ and $\vec{\rho}$ are in-plane vectors. In this case the whole wave function is seeked in the framework of adiabatic approximation:

$$\Psi(\vec{r};L) = \chi_{\vec{\rho},L}(z)\psi(\vec{\rho};L), \tag{8}$$

where the functions $\chi_{\vec{\rho},L}(z)$ and $\psi(\vec{\rho};L)$ satisfy to the equations:

$$-\frac{\hbar^2}{2m(\vec{\rho}_0;L)}\frac{d^2\chi_{\vec{\rho}_0,L}(z)}{dz^2} = E_z(\vec{\rho}_0;L)\chi_{\vec{\rho}_0,L}(z) \tag{9}$$

and

$$-\frac{\hbar^2}{2}\left\{\frac{\nabla_{\vec{\rho}}^2\psi(\vec{\rho})}{m(\vec{\rho};L)} + \left(\vec{\nabla}_{\vec{\rho}}\frac{1}{m(\vec{\rho};L)}\right)\cdot\left(\vec{\nabla}_{\vec{\rho}}\psi(\vec{\rho})\right)\right\} + \left(V(\vec{\rho},L) + \frac{\pi^2\hbar^2}{2m(\vec{\rho};L)H^2}n^2\right)\psi(\vec{\rho}) = E\psi(\vec{\rho}) \tag{10}$$

respectively.

This procedure leads to the following systems of linear equations:

$$\sum_{\vec{g}'}\left\{V_{\vec{g}-\vec{g}'}+\left[\frac{\hbar^2(\vec{k}+\vec{g}')^2}{2m}-E\right]\delta_{\vec{g},\vec{g}'}\right\}u_{\vec{g}'}=0 \tag{11}$$

for 3D SL with the Fourier transform of the potential

$$V_{g_\rho g_z}(L)=\frac{Q_e t_e X_0}{\Omega_0}\exp\left(-\frac{L^2 g^2}{4}\right)\begin{cases}\Omega_0\delta_{g_\rho,0}-2\pi\int_0^\infty z_0(\rho)I_0(g_\rho\rho)\rho d\rho & if\ g_z=0,\\ -\frac{4\pi}{g_z}\int_0^\infty \exp\left(-i\frac{g_z z_0(\rho)}{2}\right)\sin\left(\frac{g_z z_0(\rho)}{2}\right)I_0(g_\rho\rho)\rho d\rho & if\ g_z\neq 0\end{cases} \tag{12}$$

and

$$\sum_{\vec{g}'}\left\{\frac{\hbar^2}{2}m^{-1}_{\vec{g}-\vec{g}'}\left[(\vec{k}+\vec{g}')^2+(\vec{g}-\vec{g}')\cdot(\vec{k}+\vec{g}')+\left(\frac{\pi n}{h}\right)^2\right]+V_{\vec{g}-\vec{g}'}-E\delta_{\vec{g}\vec{g}'}\right\}u_{\vec{g}'}=0,\ n=1,2,... \tag{13}$$

for one layer QR SL with the Fourier transforms of the potential

$$V_{\vec{g}}=\frac{X_0 Qq}{S_0}\exp\left(-\frac{L^2g^2}{4}\right)\left\{\frac{4\sin(\pi n_x)\sin(\pi n_y)}{g_x g_y}-\frac{2\pi}{g}[R_2J_1(gR_2)-R_1J_1(gR_1)]\right\} \tag{14}$$

and the resiprocal effective mass

$$m^{-1}_{\vec{g}}=\frac{1}{S_0 m_0}\int\frac{e^{-i\vec{g}\cdot\vec{\rho}}}{0.067+0.083X(\vec{\rho},L)}d\vec{\rho}\ \square\ \frac{1}{m_0}\left(\delta_{\vec{g},0}-\frac{0.083}{0.067}\right)X_{\vec{g}}(L), \tag{15}$$

where m_0 is the free electron mass and S_0 is the area of the unite cell.

Fig. 2 illustrates the dispersion curves for the first and the second minibands in the principal directions in reciprocal space for various values of diffusion parameter for three-dimensional GSDQR SL. The general form of these curves, excepting curves in Fig. 2d, coincide with the ones obtained for bulk materials in the framework of the nearly free electrons model [23]. However due to the resonant interaction between the potential wells and the electronic wave for enough large values of k_z (small values of wavelength in z direction) the dispersion curves in k_z direction quantitatively differs from ones in other directions. In this case for enough small values of L the energy monotonically increases with the increase of k_z. However with the increase of diffusion parameter a region of energy decrease appears also in k_z direction and becomes as large as large is L. It is clear from Fig.2 that both the first and the second minibands shift to the higher energy region and broaden. Moreover the dependences on quasimomentum become more significant for all five directions. We can also conclude from the figure that the inhenced tunneling due to the diffusion leads to the significant decrease of the SL band gap.

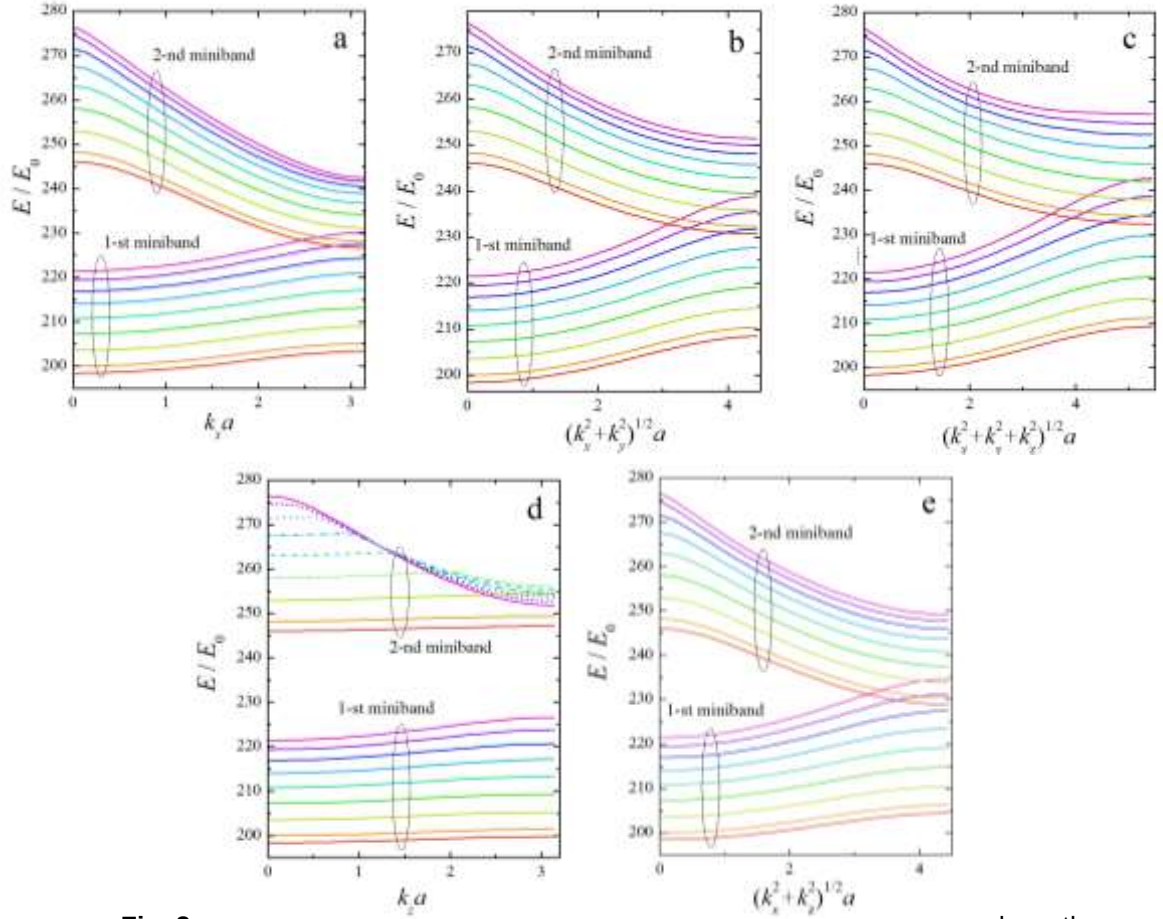

Fig. 2 The dependences of the energy of the first and the second minibands on the quasimomentum for the five principal directions in SL a) (100), b) (110), c) (111), d) (001), e) (101) and for the parameter values $R = 100$Å, $a_x = a_y = a_z = a = 200$Å. The curves corresponding to a fixed miniband are arranged from bottom to top by the values of diffusion parameter L / a = 0.01, 0.05, 0.1, 0.15, 0.2, 0.25, 0.3, 0.35, 0.4, respectively

In Fig.3 the dependences of the energy on quasimomentum for the first two minibands are presented for the one-layer QR SL. As is obvious the interdiffusion leads to the rise and to the widening of minibands. The rising of the minibands occurs due to the increase of the potential in the well regions, while the reason of widening is the electron tunneling which becomes stronger due to the smearing of the barriers. Comparing the differences between the curves 1 to 5 one can observe that the effect of interdiffusion is more significant for its intermediate values ($L = 0.05a \div 0.15a$), when the transformation of the SL potential takes place more intensively. Another peculiarity which can be observed is the stronger effect of interdiffusion on the minibands bottom comparing with its effect on the minibands top. Figs. 2a and 2c are obtained taking into account the dependence of the effective mass on the diffusion length and the coordinate according to Eq. (15), while Figs.2b and 2d correspond to the constant value of effective mass $m = 0.067m_0$. Comparison of these figures shows that the variation in the value of the energy is in the range of $3 \div 10$ mev. The values of the energy obtained by using Eq. (15) are smaller because electron in this case is heavier in the barriers region, which leads to stronger confinement and energy decrease.

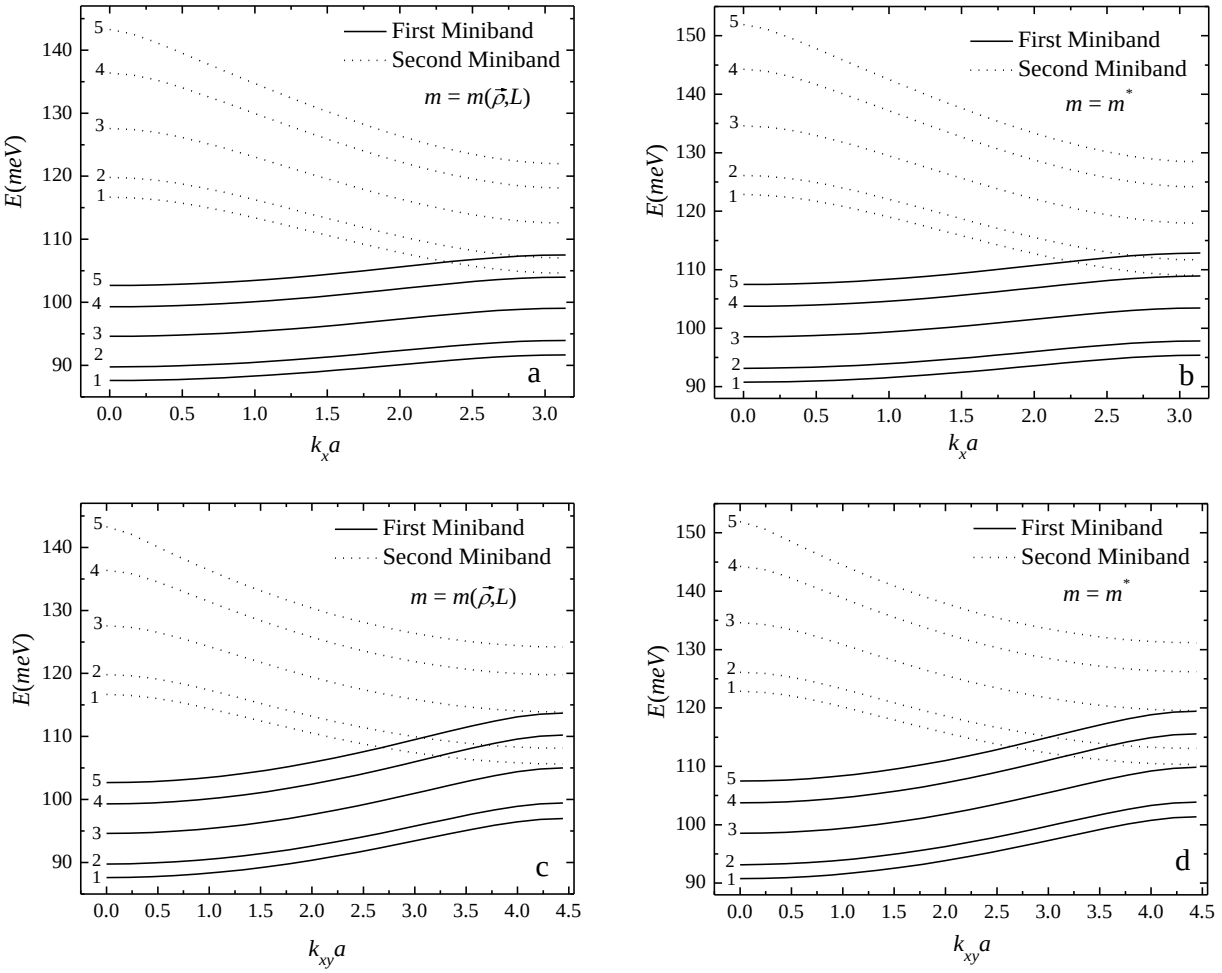

Fig. 3 The dispersion curves of the first and the second minibands of QRSL for various values of diffusion length: 1. $L = 0.01a$, 2. $L = 0.05a$, 3. $L = 0.1a$, 4. $L = 0.15a$, 5. $L = 0.2a$; $k_{xy} = (k_x^2 + k_y^2)^{1/2}$

Summarizing the effect of interdiffusion on band structure of two tipes of SLs: three-dimensional SL composed of initially cylindrical GSDQRs and one layer QR SL is studied. It is shown that the symmetry of the SL potencial superimposes on the cylindrical one of QRs due to interdiffusion. The smearing of the potential profile leads to the shift of the dispersion curves to the higher energy regions and to the minibands broadening due to the strengthening of electron tunneling. In the case of GSDQR SL the dispersion curves in k_z direction qualitatively differs from ones in other two directions even for the SL of cubic symmetry. However this difference gradually disappears with the increase of diffusion parameter. In the case of one layer QR SL the consideration of the dependence of electron effective mass on diffusion parameter and spacial coordinates leads to the decrease of electron energy up to 10meV.

The obtained results indicate to the opportunity of purposeful manipulation of structure characteristics by means of interdiffusion both quantitively and qualitatively.

ACKNOWLEDGEMENTS

This work was supported by Armenian National Science and Education Fund (ANSEF) grant nano-3334.

REFERENCES

[1] W.H. Chang, C.H. Lin, Y.J. Fu, T.C. Lin, H. Lin, S.J. Cheng, S.D. Lin, and C.P. Lee, Nanoscale Res. Lett. 5, 680 (2010).

[2] N.A. J. M. Kleemans, I. Bominaar-Silkens, V.M. Fomin, V.N. Gladilin, D. Granados, A.G. Taboada, J.M. Garcia, P. Offermans, U. Zeitler, P.C.M. Christianen, J.C. Maan, J.T. Devreese, P.M. Koenraad, Phys. Rev. Lett. 99, 146808 (2007).

[3] M. Zarenia, J.M. Pereira, F.M. Peeters, and G.A. Farias, Nano Lett. 9, 4088 (2009).

[4] A.V. Chaplik, JETP Lett. 62, 900 (1995).

[5] A.O. Govorov, S.E. Ulloa, K. Karrai, and R.J. Warburton, Phys. Rev. B 66, 081309 (2002).

[6] M.D. Teodoro, V.L. Campo, V. Lopez-Richard, E. Marega, G.E. Marques, Y.G. Gobato, F. Iikawa, M.J.S.P. Brasil, Z.Y. Abu Waar, V.G. Dorogan, Yu.I. Mazur, M. Benamara, and G.J. Salamo, Phys. Rev. Lett. 104, 086401 (2010).

[7] S. Bhowmick, G. Huang, W. Guo, C.S. Lee, P. Bhattacharya, G. Ariyawansa, and A.G.U. Perera, Appl. Phys. Lett. 96, 231103 (2010).

[8] J. Wu, Z. Li, D. Shao, M.O. Manasreh, V.P. Kunets, Zh.M. Wang, G.J. Salamo, and B.D. Weaver, Appl. Phys. Lett. 94, 171102 (2009).

[9] V.N. Mughnetsyan, A.Kh. Manaselyan, M.G. Barseghyan, A.A.Kirakosyan, J. Luminescence, 134, 24-27 (2013).

[10] H.M. Baghramyan, M.G. Barseghyan, A.A. Kirakosyan, R.L. Restrepo, C.A. Duque, J. Luminescence, 134, 594-599 (2013).

[11] A. Shahbandari, M.A. Yeranosyan, A.L. Vartanian, Superlatt. Microst. 57, 85-94 (2013).

[12] E.M. Kazaryan, V.A. Shahnazaryan, H.A. Sarkisyan, Opt. Commun. 315, 253-257 (2014).

[13] E.M. Kazaryan, V.A. Shahnazaryan, H.A. Sarkisyan, Few-Body Systems, 55, 151-158 (2014).

[14] J. Wu, D. Shao, Zh. Li, M.O. Manasreh, V.P. Kunets, Zh.M. Wang, G.J. Salamo, Appl. Phys. Lett. 95, 071908 (2009).

[15] J. Wu, Zh.M. Wang, V.G. Dorogan, Sh. Li, J. Lee, Y.I. Mazur, E.S. Kim, G.J. Salamo, Nanoscale Research Letters 8:5 (2013).

[16] Sh. Huang, Zh. Niu, Zh. Fang, H. Ni, Z. Gong et al., Appl. Phys. Lett. 89, 031921 (2006).

[17] R. Leon, S. Fafard, P.G. Piva, S. Ruvimov, Z. Liliental-Weber, Phys. Rev. B 58, R4262 (1998).

[18] T. K. Ng, H. S. Djie, S. F. Yoon, and T. Mei, J. Appl Phys. 97, 013506 (2005)

[19] A. Agarwal, M. Srujan, S. Chakrabarti, S. Krishna, J. Luminescence 143, 96 (2013).

[20] Y. Ji, W. Lu, G. Chen, X.s. Chen, Q. Wang, J. Appl. Phys. 93, 1208 (2003).

[21] J.A. Barker, E.P. O'Railly, Physica E 4, 231 (1999).

[22] O. Gunawan, H.S. Djie, B.S. Ooi, Phys. Rev. B 71, 205319 (2005).

[23] N.W. Ashkroft, N.D. Mermin. Solid State Physics. Saunders, Philadelphia, 1976.